Autophagic flux restoration enhances the antitumor efficacy of tumor infiltrating lymphocytes

Chaoting Zhang,[1] Yizhe Sun,[1] Shance Li,[1] Luyan Shen,[1] Xia Teng,[1] Yefei Xiao,[1] Nan Wu,[2] Zheming Lu [ID] [1]

[1]Laboratory of Biochemistry and Molecular Biology, Key Laboratory of Carcinogenesis and Translational Research (Ministry of Education/Beijing), Peking University Cancer Hospital & Institute, Beijing, People's Republic of China
[2]Department of Thoracic Surgery II, Key Laboratory of Carcinogenesis and Translational Research (Ministry of Education), Peking University Cancer Hospital & Institute, Beijing, People's Republic of China

Correspondence to
Dr Zheming Lu;
luzheming@bjmu.edu.cn

Dr Nan Wu;
nanwu@bjmu.edu.cn

ABSTRACT

Background Although adoptive cell therapy with tumor infiltrating lymphocytes (TILs) has mediated effective antitumor responses in several cancers, dysfunction and exhaustion of TILs significantly impair the therapeutic effect of TILs. Thus, it is essential to elucidate the exhausted characteristics of TILs and improve the antitumor effect of TILs by reversing their exhaustion. Here, we focused on the influence of autophagy on TILs in terms of T-cell activation, proliferation, and differentiation in vitro and in vivo.

Methods We first evaluated autophagy level of TILs and influence of spermidine treatment on autophagy levels of TILs. Furthermore, we assessed the proliferative potential, phenotypical characteristics, T cell receptor (TCR) repertoire and antitumor activity of TILs with and without spermidine treatment.

Results We found that autophagic flux of TILs, especially exhausted TILs that express inhibitory immunoreceptors and have impaired proliferative capacity and decreased production of cytotoxic effector molecules, was significantly impaired. The restoration of autophagic flux via spermidine treatment resulted in increased diversity of the TCR repertoire, reduced expression of inhibitory immunoreceptors (PD1, TIM3, or LAG3), enhanced proliferation and effector functions, which subsequently demonstrated the superior in vitro and in vivo antitumor activity of TILs. Our findings unveil that spermidine, as an autophagy inducer, reverses dysfunction and exhaustion of TILs and subsequently improves the antitumor activity of TILs.

Conclusions These data suggest that spermidine treatment presents an opportunity to improve adoptive TIL therapy for the treatment of solid tumors.

WHAT IS ALREADY KNOWN ON THIS TOPIC

⇒ T cell exhaustion has been shown to significantly impair the antitumor effect of tumor infiltrating lymphocytes (TILs). The autophagy plays a central role in the regulation of programs that control T-cell activation, proliferation, differentiation and survival, but it is unknown whether disturbed autophagy could correlate with dysfunction and exhaustion of TILs, and restoration of autophagy could further improve the antitumor activity of TILs.

WHAT THIS STUDY ADDS

⇒ This study found that autophagic flux of TILs, especially exhausted TILs, was significantly impaired. The restoration of autophagic flux via spermidine treatment resulted in increased diversity of the T cell receptor repertoire, reduced expression of inhibitory immunoreceptors (PD1, TIM3, or LAG3), enhanced proliferation and effector functions, which subsequently demonstrated the superior in vitro and in vivo antitumor activity of TILs.

HOW THIS STUDY MIGHT AFFECT RESEARCH, PRACTICE OR POLICY

⇒ Our findings unveil that spermidine, as an autophagy inducer, reverses dysfunction and exhaustion of TILs and subsequently improves the antitumor activity of TILs, which presents an opportunity to improve adoptive TIL therapy for the treatment of solid tumors.

INTRODUCTION

Although adoptive cell therapy (ACT) with tumor infiltrating lymphocytes (TILs) has mediated effective antitumor responses in several cancers,[1–3] T cell exhaustion, which is defined by impaired proliferative capacity, upregulation of inhibitory immunoreceptors and decreased production of cytotoxic effector molecules, has been shown to significantly impair the antitumor effect of TILs.[4] There is thus a need to study the exhausted characteristics of TILs and how to improve the therapeutic effect of TILs by reversing their exhaustion.

Macroautophagy (hereafter referred to as autophagy) is a highly conserved catabolic process that has been shown to be a crucial regulator of cell functions.[5] This process consists of the sequestration of cellular materials inside double membrane vesicles (autophagosomes), followed by fusion with lysosomes (autolysosomes) for the degradation of autophagic cargo. In T cells, autophagy not only controls organelle homeostasis[6 7] but also participates in the regulation of T cell proliferation and survival.[8 9] In addition, autophagy can also regulate T cell activation via

the controlled degradation of selective proteins involved in activation of the T cell receptor (TCR) signaling pathways, and a decrease in autophagic levels may also cause an inhibitory effect on T cell proliferation and cytokine production.[10 11]

Taken together, autophagy plays a central role in the regulation of programs that control T-cell activation, proliferation, differentiation, and survival,[12] but it is unknown whether disturbed autophagy could correlate with dysfunction and exhaustion of TILs, and restoration of autophagy could further improve the antitumor activity of TILs. Here, we present data to demonstrate that autophagic flux of TILs, especially exhausted TILs that express inhibitory immunoreceptors and have impaired proliferative capacity and decreased production of cytotoxic effector molecules, is significantly inhibited. Spermidine-enhanced autophagic flux could reverse exhaustion of TILs and subsequently improve the therapeutic efficacy of TILs against tumor cells.

RESULT
Autophagic flux of TILs, especially exhausted TILs, is significantly impaired

Lysosomal turnover of endogenous LC3-phospholipid conjugate (LC3-II) in conditions with/without autophagy inhibition has been used to examine autophagic flux.[13] To evaluate autophagic flux of peripheral T cells (PTCs), TILs and exhausted TILs, we performed biochemical analysis of autophagic markers from TILs and corresponding PTCs subjected to a series of conditions to manipulate autophagy. Western blot analysis demonstrated that LC3-II levels in TILs were significantly higher than those in PTCs under basal conditions (control). When autophagy was inhibited by chloroquine (CQ), which can prohibit LC3-II degradation by blocking the formation of autolysosomes, LC3-II levels in PTCs significantly increased, as expected, but LC3-II levels in TILs did not significantly change (figure 1A,B). To visually evaluate the LC3-II levels of TILs and PTCs, confocal microscopy showed that CQ treatment could significantly increase the LC3-II levels of PTCs but not TILs (figure 1C,D). Consistent with the western blot and confocal microscopy data, flow cytometric analysis confirmed that the LC3-II increase was significantly lower in TILs than in PTCs after CQ treatment (figure 1E,F). A similar phenomenon was observed when gated on CD8+or CD4+ T cells (online supplemental figure S1A). It is important to note that in the process of TIL generation, T cells were stimulated, and then autophagy levels could increase due to T cell activation. Therefore, to keep the autophagy levels comparable between TILs and PTCs, these data represented autophagy levels of activated TILs and PTCs. Collectively, these results indicated the accumulation of autophagosomes via defects in autophagosome–lysosome fusion and/or lysosomal degradation, suggesting autophagic flux inhibition in TILs.

Since T cell exhaustion could significantly impair the antitumor effect of TILs, it is thus necessary to evaluate autophagy levels of exhausted TILs that display a phenotype characterized by upregulation of inhibitory immunoreceptors, impaired proliferative capacity and decreased production of cytotoxic effector molecules. First, flow cytometric analysis showed that the increase in LC3-II levels in TILs expressing inhibitory immunoreceptors (PD1, TIM3, or LAG3) after CQ treatment was significantly lower than that in inhibitory immunoreceptor-negative TILs (figure 1G,H). Second, when autophagy was inhibited (CQ), the LC3-II levels of Ki67-positive TILs were significantly higher than those of Ki67-negative TILs (figure 1I,J). Third, flow cytometric analysis demonstrated that the increase in LC3-II levels in TILs secreting IFN-γ after CQ treatment was significantly higher than that in TILs without IFN-γ secretion (figure 1K,L). Similar results were found when gated on CD8+or CD4+ T cells (online supplemental figure S1B–C). In aggregate, these results indicated that TILs, especially exhausted TILs with increased inhibitory immunoreceptor expression, diminished proliferation capacity and impaired IFN-γ production ability, demonstrated severely impaired autophagic flux.

Spermidine enhances autophagic flux of TILs
Since spermidine enhances autophagic flux in multiple cell types,[14 15] we then examined whether spermidine could restore autophagic flux inhibition of TILs. Western blot analysis showed that CQ treatment significantly increased LC3-II levels in spermidine-treated TILs (sTILs) compared with TILs without spermidine treatment, indicating that spermidine restored autophagic flux in TILs (figure 2A,B). Next, to confirm whether spermidine could promote autophagic flux in live TILs, we used a mCherry-eGFP-LC3 fusion reporter system.[16] GFP fluorescence is quenched on fusion of the autophagosome with the acidified lysosome, whereas fluorescence from acid-insensitive mCherry remains until the protein is degraded (figure 2C). LC3 is hydrolyzed to expose Gly120 to generate LC3-I, which is in turn conjugated with PE to create LC3-II, enabling phagophore expansion to obtain autophagosomes.[13] An autophagy-incompetent construct including a Gly120→Ala substitution (G120A) was regarded as a negative control (online supplemental figure S2A). Confocal microscopy showed loss of GFP fluorescence in mCherry puncta in the sTILs, revealing autophagosome-lysosome fusion (figure 2D). Concurrent flow cytometric analysis further confirmed that sTILs had a greater proportion of mCherry+GFP– cells, indicating ongoing autophagic flux (figure 2E,F). Consistently, when gated CD8+or CD4+ TILs were analyzed, spermidine-treated CD8+or CD4+ TILs had enhanced autophagic flux (online supplemental figure S2B). In summary, these data indicated that spermidine enhanced autophagic flux in TILs.

Enhanced autophagic flux reverses the exhaustion of TILs
Since autophagy plays a central role in the regulation of programs that control T-cell activation, proliferation,
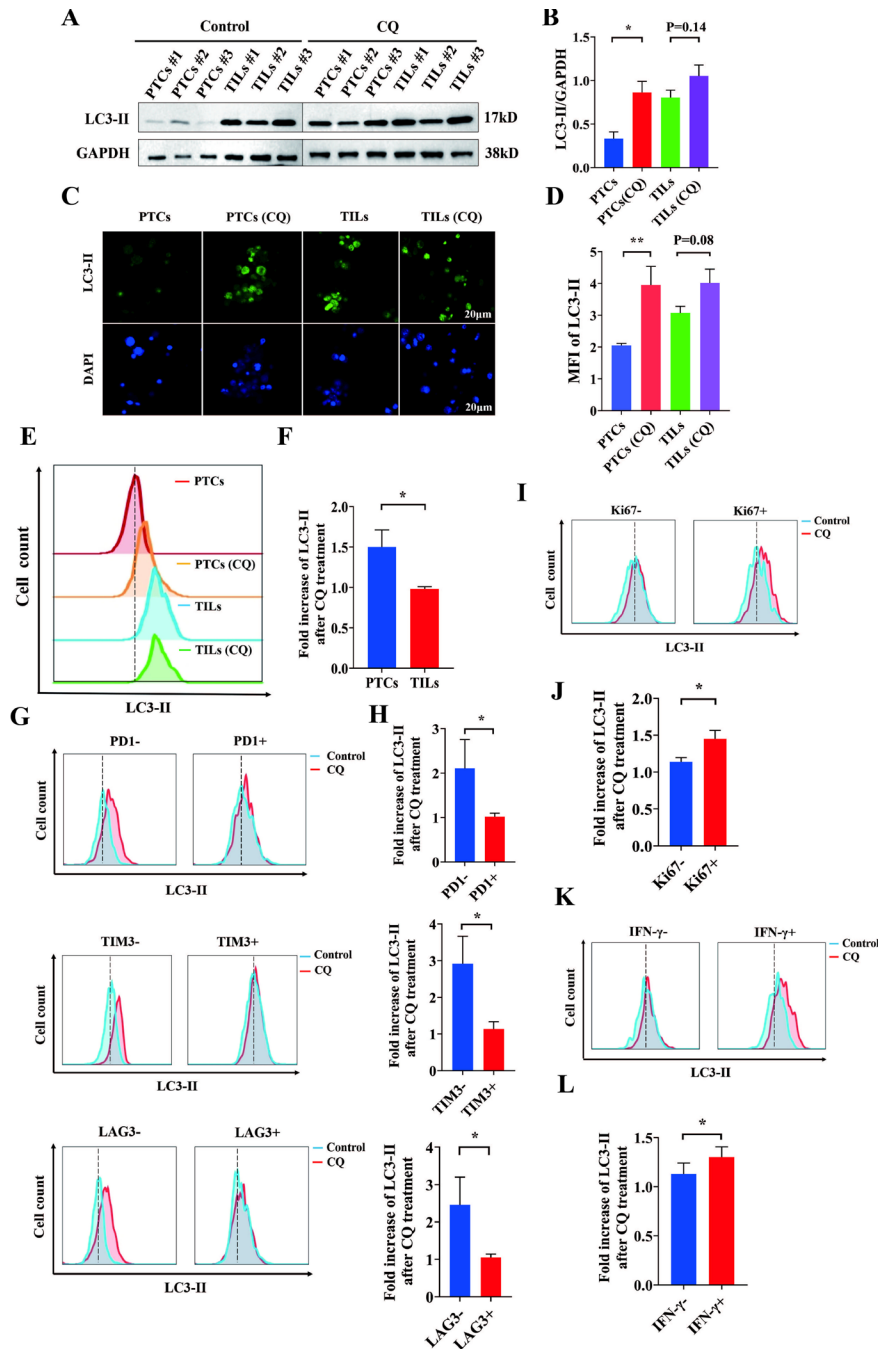
Figure 1 Autophagic flux of TILs, especially exhausted TILs, is significantly impaired. (A, B) Peripheral T cells (PTCs) and tumor-infiltrating lymphocytes (TILs) from donors treated with or without chloroquine (CQ) (50 µM; 12 hours) and LC3-II were detected by western blotting. Representative results from three PTCs and TILs were shown (A). Quantitative analysis was of the LC3-II bands was shown (n=5) (B). (C, D) Representative confocal images captured from PTCs and TILs treated with or without CQ were shown (C). The mean fluorescent intensity (MFI) of each image from different groups was statistically analyzed (n=6) (D). We used the Image J to measure the mean value for each view. To details, we chose six views for each group in ×20 magnification. And at least 12 cells determined by DAPI staining for each view, and then Image J was used to calculate the average intensity of LC3 fluorescence for all the cells in each view. (E, F) Representative flow cytometric results of LC3-II from PTCs and TILs treated with or without CQ were shown (E). The fold increases in LC3-II expression levels in PTCs and TILs after CQ treatment were summarized and shown (n=5) (F). (G, H) Representative flow cytometric results for LC3-II in PD1/TIM3/ LAG3+TILs and PD1/TIM3/LAG3- TILs with or without CQ treatment were shown (G). The fold increases in LC3-II expression levels in PD1/TIM3/LAG3+TILs and PD1/TIM3/LAG3- TILs after CQ treatment were summarized and shown (n=6) (H). (I, J) Representative flow cytometric results for LC3-II in Ki67+TILs and Ki67- TILs with or without CQ treatment were shown (I). The fold increases in LC3-II expression levels in Ki67+TILs and Ki67- TILs after CQ treatment were summarized and shown (n=4) (J). (K, L) Representative flow cytometric results for LC3-II in IFN-γ+ TILs and IFN-γ- TILs with or without CQ treatment were shown (K). The fold increases in LC3-II expression levels in IFN-γ+ TILs and IFN-γ- TILs after CQ treatment were summarized and shown (n=4) (L).
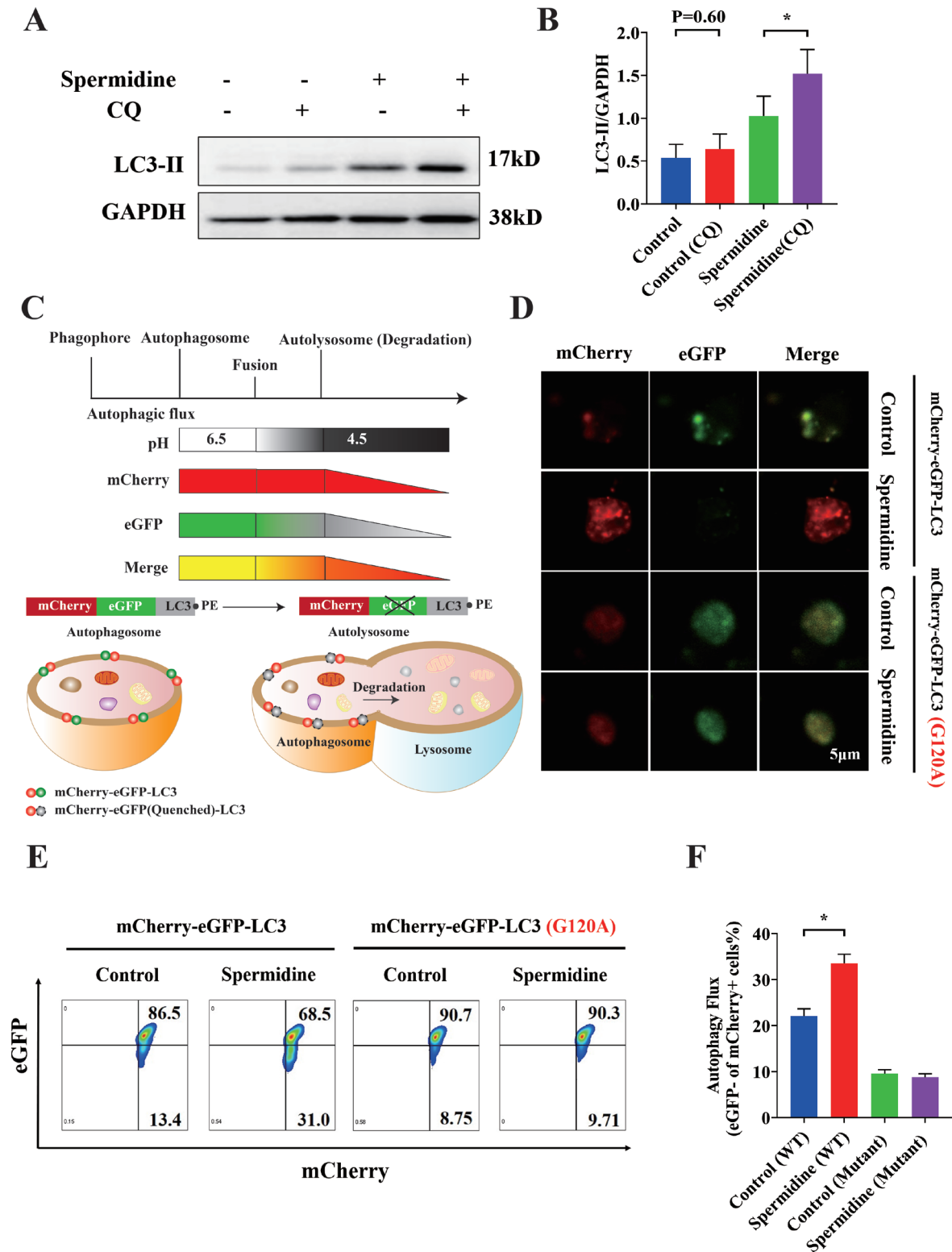
Figure 2 Spermidine enhances the autophagic flux in TILs. (A, B) Representative western blotting of LC3-II in TILs was shown. First lane indicates the TILs without spermidine or CQ treatment; second lane indicates the TILs with CQ but without spermidine treatment; third lane shows the TILs with spermidine but without CQ treatment; fourth lane shows the TILs with both spermidine and CQ treatment (A). The relative amount of LC3-II (to GAPDH) in the abovementioned four lanes was summarized (n=6) (B). (C) Diagram showing the reporting mechanism of the mCherry-eGFP-LC3 fusion protein. The pH of the autophagosome decreases from 6.5 to 4.5 on fusion with the lysosome. eGFP fluorescence was quenched in a low pH environment, while mCherry fluorescence remains until the protein was degraded (slope). (D) Representative confocal images defining the eGFP and mCherry puncta in TILs treated under the indicated conditions. (E, F) Representative flow cytometry plot (E) and quantification (F) of autophagy flux in the indicated conditions by measuring the loss of eGFP in mCherry populations (n=3). *$P<0.05$. CQ, chloroquine; TILs, tumor infiltrating lymphocytes; eGFP, enhanced green fluorescent protein.

differentiation and survival, it is essential to evaluate whether enhanced autophagic flux could reverse the exhaustion of TILs. Flow cytometric analysis demonstrated that spermidine treatment reduced the expression levels of PD1, TIM3 and LAG3, and moreover, the frequencies of double inhibitory immunoreceptors coexpressing TILs with spermidine treatment significantly declined (figure 3A–C). In addition, the viability and proliferative capacity of TILs with spermidine treatment significantly increased based on the staining status via fixable viability staining 780 (FVS780), carboxyl fluorescein succinimidyl ester (CFSE) dilution and Ki67 expression of TILs (figure 3D–I). Similar findings were observed when gated on CD8+or CD4+ T cells (online supplemental figure S3A–E). Since the TCRs expressed by TILs critically determine their capacity to specifically identify tumor antigens, the TCR repertoire diversity of TILs could significantly influence the antitumor activity of TILs. To delineate the TCR repertoire diversity of TILs in the presence or absence of spermidine, we primarily assessed the usage frequencies and distribution of V and J genes among TILs with and without spermidine treatment and found more balanced V-J usage in sTILs (figure 3J). Furthermore, we found that hyperexpanded T cell clonotypes (HECs) of sTILs occupied 11.0% of the total TCR repertoire; reciprocally, the HECs of TILs in the absence of spermidine contributed to 19.8% of the total TCR repertoires (figure 3K). To systematically and quantitatively evaluate the repertoire diversity of TILs treated or not with spermidine, we used the metric of clonality as a measure of diversity. We found that the TCR repertoire diversity of sTILs was significantly higher than that of TILs without spermidine treatment (figure 3L). Since it is difficult to determine which TILs could be tumor reactive, it is essential to sustain as many types of TILs as possible when TILs are expanded in vitro. These results suggested that sTILs could sustain TCR repertoire diversity with a stronger ability to recognize tumor antigens. In addition, we attempted to evaluate whether sTILs could significantly enhance the secretion levels of effector cytokines when they were activated. Flow cytometric analysis demonstrated that sTILs stimulated by PMA/ionomycin or OKT3 could produce more IFN-γ than TILs without spermidine treatment (figure 3M–P).

These data collectively indicated that spermidine-cultured TILs are less prone to exhaustion with lower expression levels of PD1, TIM3 and LAG3 and stronger capacities of proliferation and cytokine production and could also retain higher TCR repertoire diversity.

Restoration of autophagic flux improves the therapeutic effect of TILs

Since enhancement of autophagic flux could reverse exhaustion of TILs, it is essential to further assess whether (sTILs in the figures) had an enhanced therapeutic effect of TILs against autologous tumor cells compared with TILs without spermidine treatment. To evaluate this functionality, we first analyzed sTILs for antigen-induced

cytokine secretion on culture with autologous tumor cells. After coculture with autologous patient-derived xenograft (PDX) tumor cells (figure 4A), we found higher levels of IFN-γ in sTILs on stimulation of autologous tumor cells compared with TILs without spermidine treatment (figure 4B). Next, upregulation of degranulation ability (levels of CD107a), another benchmark of effector function, was further analyzed by flow cytometry analysis. The expression of CD107a was 18.2%±7.1 in the spermidine-untreated TILs and 33.9%±11.3 in the spermidine-treated counterparts (figure 4C,D). Consistently, when gated CD8+ or CD4+ TILs were analyzed, spermidine-treated CD8+ or CD4+ TILs expressed higher levels of CD107a than untreated CD8+ or CD4+ TILs (online supplemental figure S4A,B). The principal aim of the study was to determine whether spermidine promotes the generation of TILs with enhanced antitumor activity. Building on the reversal of exhaustion as well as improved cytokine production, we anticipated that spermidine-expanded TILs would possess enhanced antitumor activity. We found that sTILs had significantly higher cytotoxic activity against autologous tumor cells than TILs without spermidine treatment, as measured with a flow cytometry-based cytotoxicity assay in which sTILs increased PI uptake by CFSE-labeled autologous tumor cells (figure 4E,F). To test the in vivo antitumor activity, we delivered a suboptimal (5×10^6) dose of TILs intravenously into mice following subcutaneous inoculation of corresponding autologous tumor cells (figure 4G). The sTILs exhibited significantly higher antitumor activity than untreated TILs (TILs) or the control (figure 4H and online supplemental figure S5A). Moreover, flow cytometry analysis showed that significantly higher numbers of transferred T cells were detected in tumor tissue of mice infused with spermidine-treated T cells than in mice infused with untreated T cells at day 12 after tumor implantation (figure 4I,J). Meanwhile, our results also showed that transferred human T cells from tumor tissue of mice infused with spermidine-treated T cells had higher Ki67 and IFN-γ expression compared with T cells from tumor tissue of mice infused with untreated T cells at day 12 after tumor implantation (figure 4K,L). However, phenotypes of transferred human T cells from tumor tissue of mice infused TILs with and without spermidine treatment were similar at day 12 after tumor implantation (online supplemental figure S5B–F). To further evaluate the in vivo persistence of TILs and sTILs, we found more transferred human T cells from tumor tissue of mice infused with spermidine-treated T cells at day 20 after tumor implantation, but transferred human T cells from tumor tissue of mice infused with untreated T cells were rare at day 20 after tumor implantation (online supplemental figure S5G).

In aggregate, these data demonstrated that restoration of autophagic flux could significantly improve the therapeutic effect of TILs against autologous tumor cells.
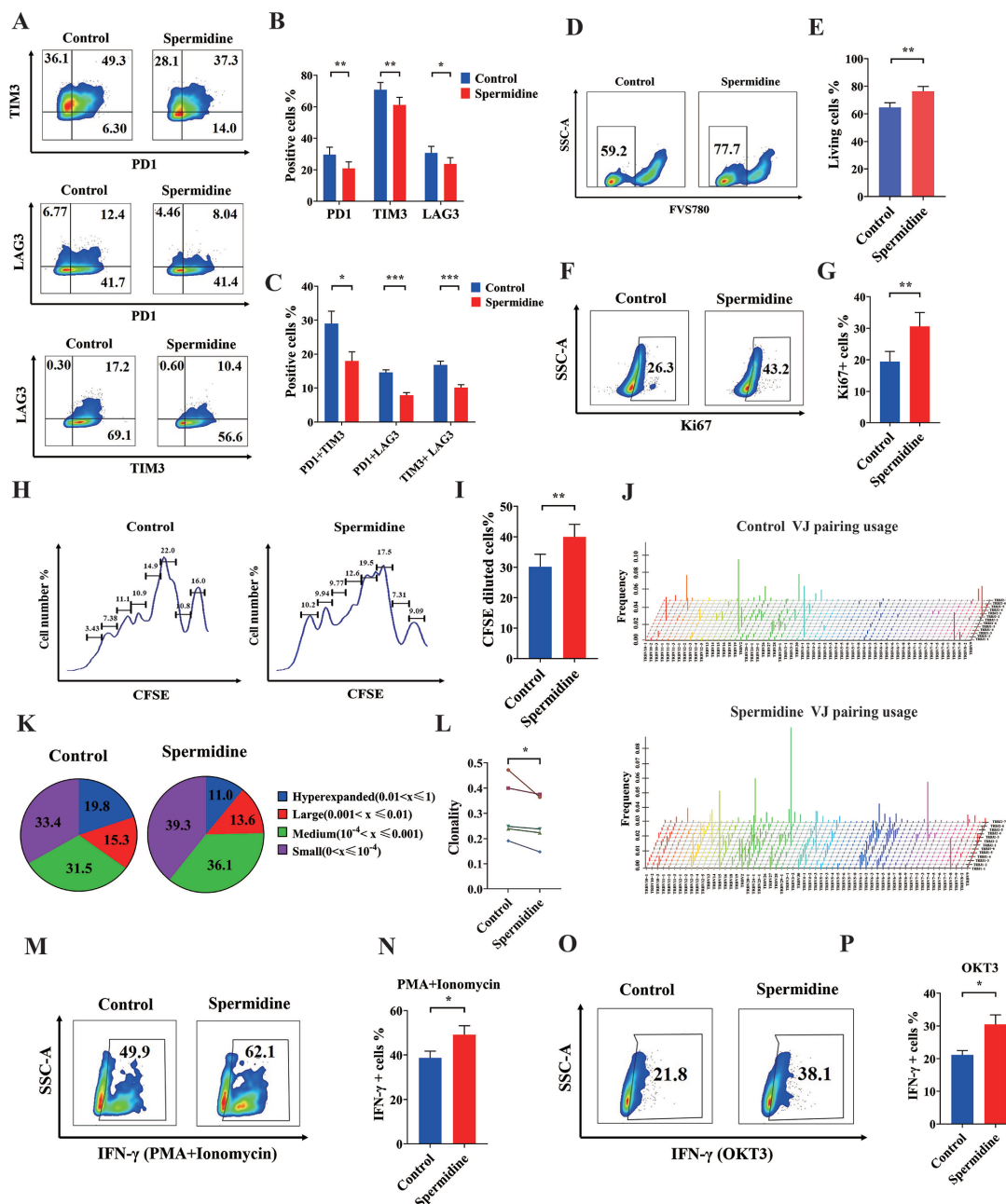
Figure 3 Dysfunction of TILs are ameliorated by spermidine. (A–C) Representative flow cytometric plots of TILs expressing inhibitory immunoreceptors (PD1, TIM3, LAG3) with or without spermidine treatment were shown (A). A statwastical summary of the proportions of PD1+, TIM3+or LAG3+TILs with or without spermidine treatment was shown (n=10) (B). Statistical summary of double-positive TILs (PD1+TIM3; PD1+LAG3; TIM3+LAG3) with or without spermidine treatment was shown (n=10) (C). (D, E) Representative flow cytometric plots demonstrating the proportions of living TILs (FVS780-) with or without spermidine treatment (D). A statistical summary of the proportions of living TILs with or without spermidine treatment was shown (n=6) (E). (F, G) Representative flow cytometric plots showing the proportions of Ki67+TILs with or without spermidine treatment (F). A statistical summary of the proportions of Ki67+TILs with or without spermidine treatment was shown (n=10) (G). (H, I) Representative flow cytometric plots of CFSE-diluted TILs with or without spermidine treatment for 7 days were shown (H). A statistical summary of CFSE-diluted TILs with or without spermidine treatment was shown (n=9) (I). (J) Representative plots of V-J pairing among TILs with or without spermidine treatment were shown. (K) Pie plots showing the frequency distribution of TCR clones from all TIL samples (n=5) with or without spermidine treatment. L, The clonality of the TCR repertoire in different TILs (n=5) with or without spermidine treatment was summarized. (M, N) Representative flow cytometric plots showing the proportions of IFN-γ+ TILs with or without spermidine treatment under PMA+ionomycin stimulation (M). The proportions of IFN-γ+ TILs with or without spermidine treatment under PMA+ionomycin stimulation were summarized (n=7) (N). (O, P) Representative flow cytometric plots demonstrating the proportions of IFN-γ+ TILs with or without spermidine treatment under OKT3 stimulation (O). The proportions of IFN-γ+ TILs with or without spermidine treatment under OKT3 stimulation were summarized (n=8) (P). *$P<0.05$, **$P<0.01$, ***$P<0.001$. CFSE, carboxyl fluorescein succinimidyl ester; TCR, T cell receptor; TILs, tumor infiltrating lymphocytes.
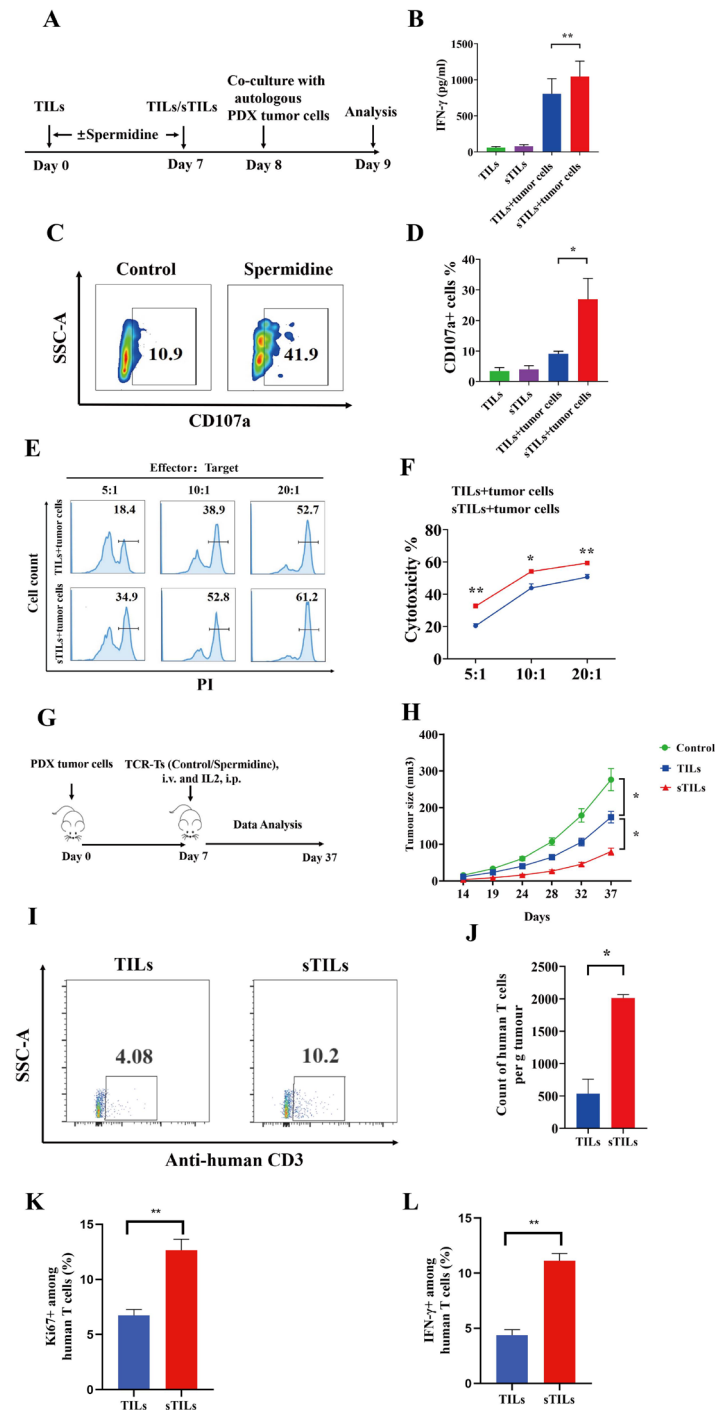
Figure 4 Restoration of autophagic flux improves the therapeutic effect of TILs in vitro and in vivo. (A) The flow diagram of in vitro coculture of TILs with or without spermidine treatment and autologous PDX tumor cells was shown. (B) IFN-γ detection in TILs and spermidine-treated TILs (sTILs) with or without coculture with autologous tumor cells was shown (n=4). (C, D) Representative flow cytometric plots showing the proportions of CD107a+TILs and sTILs (C). A statwastical summary of the proportions of CD107a+TILs and sTILs with or without coculture with autologous tumor cells was shown (n=6) (D). (E, F) Representative flow cytometric plots demonstrating the proportions of PI+cells in CFSE+autologous tumor cells cocultured with TILs or sTILs at different effector to target (E:T) ratios were shown (E). A statwastical summary of the CFSE-based cytotoxicity assay of TILs and sTILs at different E:T ratios was shown (n=3) (F). (G) The flow diagram of the in vivo adoptive experiment using TILs or sTILs was shown. (H) The growth curves of tumors in the PDX mice infused with TILs, sTILs and saline (control) were shown (n=5). The results were representative of two independent experiments. (I, J,) Representative flow cytometric plots indicating the infiltration of transferred TILs or sTILs in tumors from PDX mice was shown at day 12 after tumor implantation (I). A statistical summary of counts of transferred T cells per g tumor was shown at day 12 after tumor implantation (J) (n=3). (K, L,) Adoptively transferred TILs and sTILs in PDX tumors were analyzed for expression of Ki67 (K) and IFN-γ (L) by flow cytometry at day 12 after tumor inoculation (n=3). *P<0.05, ***P<0.001. PDX, patient-derived xenograft; PI, propidium iodide; sTILs, spermidine-treated TILs; TILs, tumor infiltrating lymphocytes.

DISCUSSION

ACT with TILs mediates effective antitumor responses in several cancers.[1–3] Since the number of TILs for clinical application could be more than 10^{10}, it is necessary for TIL in vitro expansion until the target cell number for transfer is reached. In our study, we found that spermidine treatment during TIL in vitro culture could reverse the exhaustion of TILs and further enhance the in vitro and in vivo antitumor activity of TILs due to restoration of autophagic flux.

Several pieces of evidence support that senescent T cells show autophagic flux impairment and that decreased autophagy activity has an important impact on aged T cell function.[17–19] TILs are not only generally aged T cells derived from old cancer patients but also suffer from an immunosuppressive tumor microenvironment. Thus, as expected, we found that TILs, especially exhausted TILs with increased inhibitory immunoreceptor expression, diminished proliferation capacity and impaired IFN-γ production ability, demonstrated more serious autophagic flux impairment than corresponding PTCs. Since previous studies demonstrated that spermidine could enhance autophagic flux in many cell types, including T cells,[15 20] we found that spermidine treatment not only enhanced the autophagic flux of TILs but also reversed the exhaustion of TILs and improved the therapeutic effect of TILs against tumor cells. Although no previous study reported the consequence of spermidine treatment on human TILs, several studies supported our findings that restoration of autophagy in aging mouse models could improve cell function and increase health and life span; moreover, administration of spermidine to old mice restored their ability to generate effective memory T cells.[18 21] Taken together, TILs, especially exhausted TILs, demonstrated serious autophagic flux impairment, and spermidine treatment could improve the therapeutic effect of TILs against autologous tumor cells by restoring autophagic flux, which offers a very attractive approach to enhance the antitumor activity of TILs in future clinical applications.

Although enhanced autophagic flux could reverse the exhaustion of TILs and subsequently improve the antitumor activity of TILs, how autophagy affects the T cell response remains to be further evaluated. Previous studies reported that restoring autophagy activity could improve organelle homeostasis and regulate cell metabolism, which could affect the survival and antitumor function of T cells.[22 23] Suggestive evidence for a link between loss of mitochondrial mass and upregulation of inhibitory immunoreceptors has been provided by earlier observations.[23 24] These observations suggest that TILs with restoration of autophagic flux displayed reversal of dysfunction and exhaustion and improved antitumor activity, which could be due to enhanced mitochondrial biogenesis and OXPHOS metabolism.

Autophagy is associated with not only T cell function but also the function of tumor cells. One recent study reported that autophagy inhibition of tumor cells could improve antitumor activity by restoring immunoproteasome activity and MHC class I-mediated antigen presentation of tumor cells.[25] However, our study found that TILs with enhanced autophagic flux displayed reversal of exhaustion and improved antitumor activity. Therefore, since autophagy could have different effects on TILs and tumor cells, in our study, spermidine was only added to the in vitro culture of TILs, which did not affect the function of tumor cells and could achieve better treatment outcomes.

In conclusion, autophagy plays a central role in the regulation of T cell homeostasis and function. TILs, especially exhausted TILs with increased inhibitory immunoreceptor expression, diminished proliferation capacity and impaired IFN-γ production ability, demonstrated more serious autophagic flux impairment. Enhancement of autophagic flux in TILs through spermidine treatment could reverse the exhaustion of TILs and enhance the therapeutic effect of TILs, which offers a very attractive therapeutic approach to improve adoptive TIL therapy for the treatment of solid tumors.

METHODS AND MATERIALS
Study design
This study was designed to investigate whether spermidine-enhanced autophagic flux could reverse the dysfunction and exhaustion of TILs and subsequently improve the therapeutic efficacy of TILs against tumor cells. To achieve this goal, TILs were obtained in our cancer center and became our sample reservoir. In vitro phenotypic assays were performed in the different TILs, including exhaustion and proliferation. In vitro and in vivo functional assays were performed in TILs that had the corresponding autologous PDX models, which were conducted in at least four independent samples. NOD-SCID mice with matched physical characteristics bearing PDX tumors were randomly divided into three groups: control, TILs, and sTILs. Tumor size was closely documented. Details regarding the number of independent samples for each assay are annotated in the figure legends.

Isolation and culture of PTCs and TILs
Peripheral blood mononuclear cells (PBMCs) were obtained from aged cancer patients at Beijing Cancer Hospital (Beijing, China). Isolation of PBMCs was processed by nonmobilized leukapheresis and Ficoll-Paque (GE Healthcare, UK) gradient centrifugation, and then PTCs were isolated using a Dynabeads® Untouched Human T Cells Kit (Thermo Fisher Scientific, USA) for the following experiments. Regarding TIL acquisition, patients with lung cancer providing cancer tissues provided informed consent for tissue collection and subsequent research. Details of TIL acquisition were delineated in our previous study.[26] In brief, the tumor tissues were minced into approximately 1–2 mm pieces sterilely, and each piece was placed into a well of a 24-well plate with T cell culture medium. The culture medium was mainly from X-VIVO 15 serum-free medium (Lonza, USA) supplemented with GlutaMAX (Thermo Fisher, USA), IL2 (50 U/mL; Peprotech, USA), IL-7 (10 ng/mL; Peprotech, USA), IL-15 (10 ng/mL, Peprotech, USA),

OKT3 antibody (50 ng/mL; ACRO, USA), and anti-CD28 antibody (1 µg/mL; T&L Biotechnology, China). The tumor piece was cultured in a 37 °C incubator with 5% CO_2, and TILs infiltrating the tumor piece proliferated under stimulation. Then, TILs were collected and cryopreserved in liquid nitrogen for the following experiments when TILs reached a cell density of approximately 1×10^6 per well. The characteristics of TILs were delineated in online supplemental table S1.

TILs in the control group were resuspended and cultured in T cell culture medium as described above for up to 7 days, and spermidine (10 µM) (Cayman Chemical, USA) was added to the culture of TILs in the experimental groups for 7 days, followed by the identification of multiple parameters and phenotypes.

Cell staining and flow cytometry

TILs were collected into tubes, and a washing step was performed with phosphate-buffered saline (PBS) solution. First, fixable viability stain 780 (FVS780) was used to stain the cells protected from light for 15 min at room temperature. Then, antibodies against membrane molecules, including CD3 (UCHT1), CD4 (RPA-T4), CD8 (RPA-T8), PD1(EH12.1), TIM3 (7D3), and LAG3 (T47-530) were used to stain cells for 15 min at room temperature without light exposure.

For intracellular molecules, cells were fixed and permeabilized using fixation and permeabilization buffer (BD Biosciences) for 15 min at room temperature. After two washes with perm/wash buffer (BD Biosciences), the cells were mixed with intracellular antibodies in wash buffer including Ki67 (B56) and IFN-γ (B27) for 15 min without light exposure, and flow cytometric analysis was conducted after two washes with PBS. Specifically, intracellular IFN-γ detection required prior overnight operation by GolgiPlug, a protein transporter inhibitor (BD Biosciences, USA). The work guideline of GolgiPlug was 1 µL of 1 mL medium (approximately 1×10^6 cells) and required thorough mixing.

For CD107a staining, CD107a (H4A3) antibody combined with GolgiPlug was mixed and then incubated with the cells overnight, and flow cytometric analysis was performed after cell viability and other surface marker staining.

For LC3 cytometric staining, 1-hour fixation and permeabilization against exposure to light at room temperature was required after FVS780 staining. Then, the cells were washed twice with perm/wash buffer, and Alexa Fluor 488-labeled LC3 antibody (D11, Cell Signaling Technology, USA) in perm/wash buffer was mixed with the fixed cells at a dilution of 1:50 for 1 hour at room temperature. After centrifugal discarding of the LC3 antibody and washing twice with PBS, the surface markers mentioned above were used to stain the cells as described above. Cells were washed twice with PBS prior to flow cytometric analysis.

Cells were acquired on BD FACSAria and BD FACS-Celesta SORP. Data collected were analyzed further by FlowJo V.10.6.2 software (BD Biosciences, USA)

CFSE dilution assay

Cells in the abovementioned T cell medium were mixed with 2 µM CellTrace_ CFSE (Thermo Fisher, USA) for 30 min in a 37°C incubator without light exposure, and then complete medium with fetal bovine serum (FBS) (Corning, USA) was added and mixed with the cells for 10 min to stop the staining process. Cells were then pelleted, and the supernatant was removed. Finally, the cells were resuspended in T cell medium after one wash with PBS, with and without spermidine treatment. Cells after 7 days of incubation without light exposure were collected for flow cytometric analysis. Proliferation histogram fitting was achieved by FlowJo V.10.6.2 software (BD Biosciences, USA)

Immunofluorescence assay

For LC3 staining, cells were collected and pelleted, and then fix & perm buffer (BD Biosciences USA) was mixed with the cells for 20 min at room temperature. Triton X-100 (0.1%) in PBS was added to the cells for further permeabilization for 15 min after washing. Then, 5% BSA in PBS was incubated with the cells for 1 hour to block the nonspecific sites, and Alexa Fluor 488-labeled LC3 antibody (Cell Signaling Technology, USA) at a dilution of 1:100 was incubated with the cells for 1 hour at room temperature without light exposure. After two washes of the cells, the cells were resuspended in 90% glycerol in PBS and placed in a confocal dish for subsequent observation.

Lentivirus construction and transduction of TILs

The sequences of wild-type and mutant mCherry-eGFP-LC3 were obtained from the Addgene database, and the plasmids were synthesized by GenScript Bioscience Company (Nanjing, China). The target fragment in the plasmid was cloned into the lentiviral vector named pCDH-EF1-MCS-T2A-Puro with two restriction sites of ECOR I and BamH I. Then, the lentivirus was generated by cotransduction of 293 FT cells with lentivector and packaging plasmids using PEI MAX 40000 (Polysciences, USA). The lentiviral supernatants were harvested at 48 and 72 hours after transfection and concentrated using ultracentrifugation at 20 000 g for 90 min at 4°C.[27 28] TILs were cultured and stimulated with T cell culture medium with OKT3 and anti-CD28 antibodies for 1 day. Activated TILs were transduced by concentrated lentivirus with 8 µg/mL polybrene (Sigma-Aldrich, USA). Spermidine was administered to the transduced cells after 2 days. Flow cytometry was conducted after 7 days focusing on mCherry and eGFP.

Production of cell lysates and Western Blotting

Cells were pelleted and washed by PBS. Cell pellets were pipetted and lysed in loading buffer with β-mercaptoethanol for 15 min on ice. Cell insoluble debris was removed by centrifugation, and 10 min of water boiling at 95°C was followed. Cell lysates were loaded on 15% SDS-PAGE gels and separated by electrophoresis followed by transfer into polyvinylindene fluoride (Bio-Rad, USA) membranes preactivated

by menthol. After transfer, the membranes were blocked with 5% skim milk in 0.1% Tween 20/TBS (TBST) for 2 hours at room temperature and then incubated overnight at 4°C with specific primary antibodies at a dilution of 1:1000, mainly anti-LC3B (Cell Signaling Technology, USA) and anti-GAPDH (ZSGB Biotechnology, China), in our study. The membranes were washed with TBST three times and incubated with horseradish peroxidase (HRP)-conjugated goat anti-mouse or rabbit secondary antibody (1:2000) (ZSGB Biotechnology, China) for 1 hour. After three washes with TBST, membranes were detected by chemiluminescence using the Enhanced Chemiluminescence Detection Kit-HRP (Biological Industrials, Israel). Images were captured by a Champchemi610 (Sagecreation, China). Western images were calculated and analyzed by ImageJ, which is the open source. The relative amount of the specific protein was determined by the ratio of its gray value to the counterpart of GAPDH.

High-throughput sequencing of TCRβ

Details of TCRβ sequencing were delineated in our previous studies.[29 30] Briefly, the CDR3 region of the TCRβ chain was amplified using multiplex PCR and sequenced using the Illumina HiSeq 2500 platform (MyGenostics, China) from the genomic DNA of each sample. The CDR3 region of the TCRβ chain was identified based on the definition established by the International ImMunoGeneTics collaboration.[31] Sequencing reads that did not match the structure of the CDR3 region were not included in the analysis. A standard algorithm was applied to identify V, D, and J segments contributing to the CDR3 region of the TCRβ chain.[31] Since CDR3 sequences, including frameshifts or stop codons, are unlikely to translate into a functional protein, only productive reads that did not include frameshifts or stop codons were used for downstream analyses. To quantify the diversity of the TCR repertoire for each sample, we used the clonality index, which is defined as 1− (Shannon's entropy)/log2 (number of productive unique reads) with values ranging from 0 (most diverse) to 1 (least diverse).

In vitro coculture with autologous PDX tumor cells

TILs were treated with or without spermidine for 7 days and stimulated with OKT3 and anti-CD28 antibodies. Then, the medium with the OKT3 and anti-CD28 antibodies was removed and replaced with X-VIVO 15 serum-free medium overnight.

PDX tumors from NOD-SCID mice were resuspended in X-VIVO 15 medium and centrifuged. The pellets were resuspended in X-VIVO 15 medium in a homogenizer tube and fully dissociated using a tumor dissociation kit (Miltenyi Biotech, USA) by placing them in a gentleMACS Octo dissociator (Miltenyi Biotech, USA) for 30 min. Following centrifugation, resuspension in fresh medium was conducted. After cell counting using Countess II (Invitrogen, USA), the TILs and tumor cells were cocultured in a 96-well plate in a 1:1 ratio of effector cells:target cells (E:T) for 24 hours. Then, the cells were collected for the flow cytometric analysis of cell surface markers by the protocol described above, and simultaneously, the supernatants were collected for cytokine detection, which is described as follows.

Cell cytokines measurement

The previous steps of coculture were described above, and IFN-γ was measured in the coculture supernatants by a Human Th1/Th2/Th17 Kit (RUO) Brand BD^M Cytometric Bead Array (BD Biosciences, USA). Fifty microliters of each sample were mixed with mixing beads consisting of capture beads for specific cytokines and PE-labeled detection reagent. In addition, a 3-hour incubation was required. After washing and resuspension with 300 µL of washing buffer, the samples were analyzed by an Accuri C6 flow cytometer (BD Biosciences, USA), and the concentration of each cytokine was calculated according to the standard samples. The intensity of fluorescence was analyzed by FCAP Array V.3 software (BD Biosciences, USA).

In vitro cell toxicity assay

We used the CFSE-based cell cytotoxicity assay to measure the efficacy of the T cells. The process of PDX tumors was described above, and the dissociated tumor cells were stained with 2 µM CFSE for 30 min followed by PBS washing and staining stopped with FBS-containing medium for 10 min. The CFSE-stained tumor cells were cocultured with T cells at E:T ratios of 5:1, 10:1 and 20:1 for 6 hour in a 37°C incubator. After coculture, 1 µg/mL propidium iodide (BD Biosciences, USA) was added to stain the target cells for 15 min at room temperature, and then the samples were analyzed by an Accuri C6 Flow Cytometer (BD Biosciences, USA).

In vivo adoptive TIL experiments

TILs treated with and without spermidine for 7 days were collected and pelleted. NOD-SCID mice were separated into a control group without TIL infusion, a TIL group with TIL infusion and a sTIL group with sTIL infusion. NOD/SCID mice were used to establish PDX approved by the Institutional Review Board of the Peking University School of Oncology, China. The tumor tissue was cut into very small tumor fragments (tumor tissue suspension). And then PDX model was established by implanting tumor tissue suspension mixed with matrigel subcutaneously into immunodeficient NOD-SCID mice to generate PDX model. All procedures were performed under sterile conditions at Peking University Cancer Hospital specified-pathogens free facility and carried out in accordance with the Guide for the Care and Use of Laboratory Animals of the NIH. Next, 5×10^6 TILs were intravenously infused into tumor-bearing NOD-SCID mice simultaneously with intraperitoneal injection of 3000 UI IL2 on day 7. The tumor volumes were observed by measuring tumor diameters at 14, 19, 24, 28, 32, and 37 days.

Statistical analysis

Statistical analyses were performed with Stata V.11.0 for Windows (StataCorp) using two-tailed unpaired or paired Student's t-test, Wilcoxon matched-pairs signed-ranks

test, and one-way analysis of variance. In all cases, statistical significance was considered when p<0.05. Error bars show the mean±SE of the mean (SEM), and p values are represented as follows: *p<0.05, **p<0.01, ***p<0.001.

Data access

Raw TCRβ chain sequencing data were submitted to the Sequence Read Archive (BioProject No. PRJNA731288).

ORCID iD
Zheming Lu http://orcid.org/0000-0003-3775-9435

REFERENCES

1 Dudley ME, Wunderlich JR, Yang JC, *et al*. Adoptive cell transfer therapy following non-myeloablative but lymphodepleting chemotherapy for the treatment of patients with refractory metastatic melanoma. *J Clin Oncol* 2005;23:2346–57.
2 Stevanović S, Draper LM, Langhan MM, *et al*. Complete regression of metastatic cervical cancer after treatment with human papillomavirus-targeted tumor-infiltrating T cells. *J Clin Oncol* 2015;33:1543–50.
3 Tran E, Turcotte S, Gros A, *et al*. Cancer immunotherapy based on mutation-specific CD4+ T cells in a patient with epithelial cancer. *Science* 2014;344:641–5.
4 Wherry EJ, Kurachi M. Molecular and cellular insights into T cell exhaustion. *Nat Rev Immunol* 2015;15:486–99.
5 Boya P, Reggiori F, Codogno P. Emerging regulation and functions of autophagy. *Nat Cell Biol* 2013;15:713–20.
6 Jia W, He Y-W. Temporal regulation of intracellular organelle homeostasis in T lymphocytes by autophagy. *J Immunol* 2011;186:5313–22.
7 Pua HH, Guo J, Komatsu M, *et al*. Autophagy is essential for mitochondrial clearance in mature T lymphocytes. *J Immunol* 2009;182:4046–55.
8 Pua HH, Dzhagalov I, Chuck M, *et al*. A critical role for the autophagy gene Atg5 in T cell survival and proliferation. *J Exp Med* 2007;204:25–31.
9 Li C, Capan E, Zhao Y, *et al*. Autophagy is induced in CD4+ T cells and important for the growth factor-withdrawal cell death. *J Immunol* 2006;177:5163–8.
10 Paul S, Kashyap AK, Jia W, *et al*. Selective autophagy of the adaptor protein Bcl10 modulates T cell receptor activation of NF-κB. *Immunity* 2012;36:947–58.
11 Jia W, He M-X, McLeod IX, *et al*. Autophagy regulates T lymphocyte proliferation through selective degradation of the cell-cycle inhibitor CDKN1B/p27Kip1. *Autophagy* 2015;11:2335–45.
12 Botbol Y, Guerrero-Ros I, Macian F. Key roles of autophagy in regulating T-cell function. *Eur J Immunol* 2016;46:1326–34.
13 Klionsky DJ. Guidelines for the use and interpretation of assays for monitoring autophagy. In: *Autophagy, 24*. 3rd ed, 2016: 1–222.
14 Madeo F, Eisenberg T, Pietrocola F, *et al*. Spermidine in health and disease. *Science* 2018;359. doi:10.1126/science.aan2788. [Epub ahead of print: 26 Jan 2018].
15 Eisenberg T, Knauer H, Schauer A, *et al*. Induction of autophagy by spermidine promotes longevity. *Nat Cell Biol* 2009;11:1305–14.
16 Vodnala SK, Eil R, Kishton RJ, *et al*. T cell stemness and dysfunction in tumors are triggered by a common mechanism. *Science* 2019;363. doi:10.1126/science.aau0135. [Epub ahead of print: 29 03 2019].
17 Phadwal K, Alegre-Abarrategui J, Watson AS, *et al*. A novel method for autophagy detection in primary cells: impaired levels of macroautophagy in immunosenescent T cells. *Autophagy* 2012;8:677–89.
18 Puleston DJ, Zhang H, Powell TJ, *et al*. Autophagy is a critical regulator of memory CD8(+) T cell formation. *Elife* 2014;3. doi:10.7554/eLife.03706. [Epub ahead of print: 11 Nov 2014].
19 Mittelbrunn M, Kroemer G. Hallmarks of T cell aging. *Nat Immunol* 2021;22:687–98.
20 Carriche GM, Almeida L, Stüve P, *et al*. Regulating T-cell differentiation through the polyamine spermidine. *J Allergy Clin Immunol* 2021;147:e311:335–48.
21 Fernández Álvaro F, Sebti S, Wei Y, *et al*. Disruption of the beclin 1-BCL2 autophagy regulatory complex promotes longevity in mice. *Nature* 2018;558:136–40.
22 Sena LA, Li S, Jairaman A, *et al*. Mitochondria are required for antigen-specific T cell activation through reactive oxygen species signaling. *Immunity* 2013;38:225–36.
23 Scharping NE, Menk AV, Moreci RS, *et al*. The tumor microenvironment represses T cell mitochondrial biogenesis to drive intratumoral T cell metabolic insufficiency and dysfunction. *Immunity* 2016;45:374–88.
24 van Bruggen JAC, Martens AWJ, Fraietta JA, *et al*. Chronic lymphocytic leukemia cells impair mitochondrial fitness in CD8+ T cells and impede CAR T-cell efficacy. *Blood* 2019;134:44–58.
25 Deng J, Thennavan A, Dolgalev I, *et al*. ULK1 inhibition overcomes compromised antigen presentation and restores antitumor immunity in LKB1 mutant lung cancer. *Nat Cancer* 2021;2:503–14.
26 Tan Q, Zhang C, Yang W, *et al*. Isolation of T cell receptor specifically reactive with autologous tumour cells from tumour-infiltrating lymphocytes and construction of T cell receptor engineered T cells for esophageal squamous cell carcinoma. *J Immunother Cancer* 2019;7:232.
27 Zhang C, Tan Q, Li S, *et al*. Induction of EBV latent membrane protein-2A (LMP2A)-specific T cells and construction of individualized TCR-engineered T cells for EBV-associated malignancies. *J Immunother Cancer* 2021;9:e002516.
28 Zhang C, Palashati H, Rong Z, *et al*. Pre-depletion of TRBC1+ T cells promotes the therapeutic efficacy of anti-TRBC1 CAR-T for T-cell malignancies. *Mol Cancer* 2020;19:162.
29 Zhang C, Ding H, Huang H, *et al*. TCR repertoire intratumor heterogeneity of CD4+ and CD8+ T cells in centers and margins of localized lung adenocarcinomas. *Int J Cancer* 2019;144:818–27.
30 Chen Z, Zhang C, Pan Y, *et al*. T cell receptor β-chain repertoire analysis reveals intratumour heterogeneity of tumour-infiltrating lymphocytes in oesophageal squamous cell carcinoma. *J Pathol* 2016;239:450–8.
31 Yousfi Monod M, Giudicelli V, Chaume D, *et al*. IMGT/JunctionAnalysis: the first tool for the analysis of the immunoglobulin and T cell receptor complex V-J and V-D-J junctions. *Bioinformatics* 2004;20 Suppl 1:i379–85.